Cation-ligand hybridization for stoichiometric and reduced TiO_2 (110) surfaces determined by resonant photoemission

Zhaoming Zhang, Shin-Puu Jeng, and Victor E. Henrich
Surface Science Laboratory, Department of Applied Physics, Yale University, New Haven, Connecticut 06520
(Received 9 August 1990; revised manuscript received 16 December 1990)

We have performed a resonant photoemission study on both stoichiometric and reduced TiO_2 (110) surfaces using synchrotron radiation. A resonant enhancement of the O $2p$ valence-band photoemission intensity is observed for both stoichiometric and reduced TiO_2 surfaces as the photon energy is swept through the Ti $3p \rightarrow 3d$ optical transition energy, which indicates a strong hybridization between the oxygen and titanium ions. Compared to the stoichiometric surface, the amplitude of the resonance is smaller for the reduced surface. In addition, the reduced surface has higher emission intensity from the O $2p$ bonding orbitals and lower emission intensity from the nonbonding orbitals. For both stoichiometric and reduced surfaces, the intensity of emission from the O $2p$ bonding orbitals resonates more than that from the O $2p$ nonbonding orbitals, and the resonance profile for the nonbonding orbitals maximizes at a higher photon energy than that for the bonding orbitals. The resonant enhancement of the O $2p$ bonding orbitals is consistent with theoretical calculations, which predict that the O $2p$–Ti $3d$ hybridization involves primarily those O $2p$ orbitals. The energy dependence of the resonant enhancement for the O $2p$ nonbonding orbitals suggests that it results predominantly from resonant processes involving Ti $3p \rightarrow 4s$ excitation at the surface.

I. INTRODUCTION

Recently there has been a great deal of interest, both theoretical and experimental, in resonant photoemission from the $3d$ transition-metal components.[1] While the resonant photoemission process for the heavy $3d$ transition-metal compounds ($Z > 25$) has been interpreted successfully by means of configuration interaction (CI) cluster calculations which take into account ligand-to-metal charge transfer,[2] the resonance mechanism for the light $3d$ transition-metal compounds is not as well understood.

In resonant photoemission, the amplitude of features in the spectra change as the photon energy is tuned through an optical-absorption edge of one of the constituent atoms; in the work reported here the photon energy is tuned through the $3p \rightarrow 3d$ optical-absorption edge of titanium. The resonant behavior is due to interference between the direct photoemission process:

$$3p^6 3d^n + h\nu \rightarrow 3p^6 3d^{n-1} + e^- ,$$

and the photoabsorption process:

$$3p^6 3d^n + h\nu \rightarrow [3p^5 3d^{n+1}]^*$$

(where the asterisk denotes an excited state), followed by a super-Coster-Kronig decay into a continuum state (autoionization process):

$$[3p^5 3d^{n+1}]^* \rightarrow 3p^6 3d^{n-1} + e^- .$$

Since the resonant process involves a $3p \rightarrow 3d$ transition on the cations, only features associated with the cation $3d$ orbitals are expected to resonate.[1] However, in transition-metal oxides it has been found that features in the O $2p$ valence band resonante as well,[3–7] even though no optical-absorption transitions for the oxygen ions exist in the photon energy range used. The valence-band resonant behavior is thought to result from hybridization between the cations and their oxygen ligands involved in solid-state bonding.[1] Stoichiometric TiO_2 has a nominally Ti^{4+} $3d^0$ electronic configuration. However, the surface can be reduced by ion bombardment to creat O-vacancy defects and partially populate the $3d$ orbitals of the surface cations.[8,9] It is therefore an excellent material in which to study valence-band resonant photoemission as a function of d-orbital population in order to determine the nature of the cation-ligand hybridization.

In this paper we report the results of angle-integrated resonant photoemission experiments on both stoichiometric and reduced TiO_2 (110) surfaces using synchrotron radiation. Section II describes the experimental procedure and sample preparation. In Sec. III the results of ultraviolet photoemission spectroscopy (UPS) and resonant photoemission for photon energies in the vicinity of the Ti $3p \rightarrow 3d$ optical-absorption edge are presented and discussed in terms of the available calculations. Finally, a brief summary is given in Sec. IV.

II. EXPERIMENTAL PROCEDURE

All experiments were performed on beamline U14 at the National Synchrotron Light Source (NSLS) at Brookhaven National Laboratory using photon energies between 30 and 80 eV from a plane grating monochromator. The photoemission spectra were taken in a semi-angle-integrated mode using a double-pass cylindrical mirror analyzer (CMA) operated at 23 eV pass energy. The energy resolution, due to the combined resolving powers of the CMA and monochromator, was about 0.4

eV in the photon energy range used. The p-polarized photons were incident onto the sample at an angle of 45° with respect to the surface normal. The CMA axis was perpendicular to the incident photon beam in the scattering plane. The pressure in the analysis chamber was about 5×10^{-10} Torr during the measurements. All the spectra presented here have been referenced to the Fermi level E_F, which is determined from the UPS spectrum of a clean gold foil. The spectra taken were normalized to the incoming photon flux using a Au-coated grid flux monitor situated in the path of the beam. The background at any point, due to inelastically scattered electrons, is assumed to arise solely from the scattering of electrons of higher kinetic energy and is thus taken to be proportional to the integrated photoelectron intensity for all higher kinetic energies. Integrated backgrounds determined in this way were subtracted from the O $2p$ valence-band photoemission spectra. Linear backgrounds were subtracted from the spectra of the defect-induced Ti $3d$ states close to the Fermi level since the background is very low in that region. Resonance profiles were measured by taking a series of energy distribution curves (EDC's) at different photon energies and integrating the area above background under a given emission feature.

The single-crystal rutile TiO_2 (110) sample was oriented to within 0.5° using x-ray Laue diffraction and cut into a rectangular slab of $10\times5\times1.5$ mm^3. The crystal was mechanically polished, etched in concentrated H_2SO_4, and then rinsed with distilled water. The bulk of the sample was slightly reduced in the analysis chamber by heating it to 823 K for about 15 h in UHV. The reduced sample was gray in color, corresponding to about 10^{17}–10^{18} oxygen vacancies per cm^3 in the bulk. This reduction is sufficient to eliminate any sample charging during spectroscopic measurements. The stoichiometric TiO_2 (110) surface was prepared by Ar-ion bombardment for 5 min at 2 keV followed by 25 min at 0.5 keV; the sample was then annealed at 823 K for 30 min in 1×10^{-7}-Torr O_2. Good (1×1) low-energy electron diffraction (LEED) patterns were obtained from the (110) surfaces prepared in this way. The reduced surface was produced by the same Ar-ion bombardment procedure above, but without subsequent annealing. Auger electron spectroscopy was used to verify the cleanness of both surfaces.

III. RESULTS AND DISCUSSION

The angle-integrated photoemission spectra for stoichiometric and reduced TiO_2 (110) surfaces at different photon energies are shown in Figs. 1 and 2, respectively. Both surfaces exhibit a broad feature between about 3.5 and 9.5 eV below E_F, which corresponds to the predominantly O $2p$ valence band. In the rutile structure each Ti atom is surrounded by a slightly distorted octahedron of O atoms.[10] According to the molecular orbital description of the $(TiO_6)^{8-}$ cluster, the oxygen valence band is composed of a variety of orbitals: t_{1g}, t_{2u}, $3t_{1u}$, $1t_{2g}$, $2t_{1u}$, $2e_g$, and $2a_{1g}$.[11] Among these the $1t_{2g}$ and $2e_g$ orbitals are π and σ bonding to the Ti $3d$

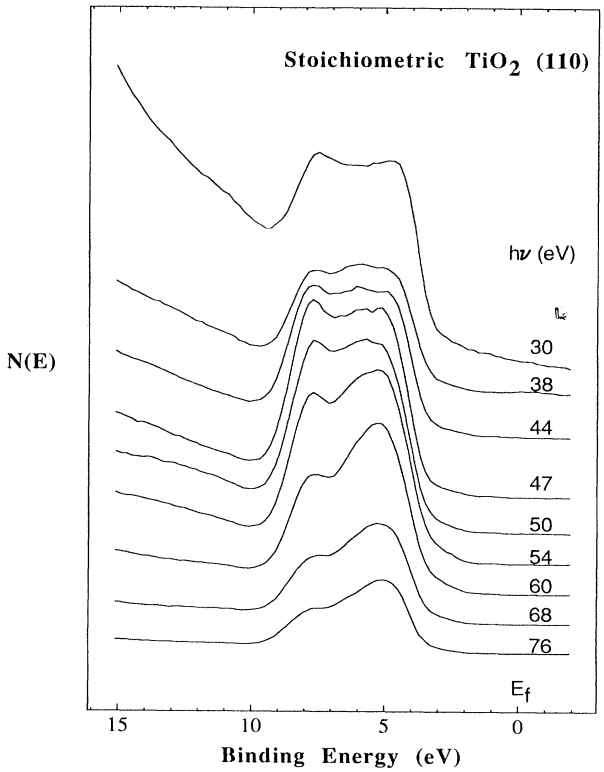

FIG. 1. Series of angle-integrated UPS spectra from stoichiometric TiO_2 (110) taken for photon energies between 30 and 76 eV.

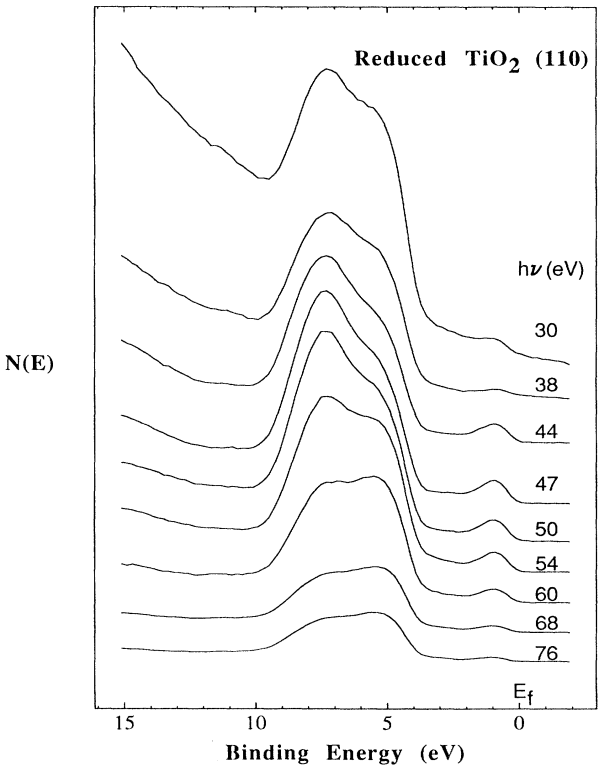

FIG. 2. Series of angle-integrated UPS spectra from reduced TiO_2 (110) taken for photon energies between 30 and 76 eV.

states,[11] with 12% and 21% charge density at each Ti site, respectively.[12] The higher-binding-energy region of the oxygen valence band consists of these bonding orbitals, while the nonbonding orbitals comprise the lower-binding-energy region of the valence band. When the stoichiometric TiO_2 (110) surface is bombarded by inert gas ions, O-vacancy defects are created in the surface region;[8,9] these defect sites must be negatively charged in order to maintain local charge neutrality. The negative charge is shared by the Ti ions adjacent to the vacancy, partially populating their $3d$ orbitals.[8,9] These $3d$ electrons are seen in Fig. 2 as a band of states lying in the bulk-band-gap region just below E_F.

A. Resonant photoemission in stoichiometric TiO_2

The photon energy dependence of the total O $2p$ emission (area above an integrated background) for a stoichiometric TiO_2 (110) surface is shown in Fig. 3. A broad resonant peak is observed in the Ti $3p \rightarrow 3d$ core excitation energy range (the Ti $3p \rightarrow 3d$ absorption threshold measured optically is at 45.9 eV for Ti metal[13]). When the photon energy is greater than the $3p \rightarrow 3d$ excitation threshold, Ti $3p$ electrons are excited into the initially empty $3d$ band:

$$\text{Ti } 3p^6 3d^0 + h\nu \rightarrow \text{Ti } [3p^5 3d^1]^* \ .$$

Due to the absence of any intra-atomic Auger decay channel, the $[3p^5 3d^1]^*$ excited state can only decay nonradiatively by energy transfer to the oxygen valence-band electrons through Ti $3d$–O $2p$ hybridization:

$$\text{Ti } [3p^5 3d^1]^* + \text{O } 2p^6 \rightarrow \text{Ti } 3p^6 3d^0 + \text{O } 2p^5 + e^- \ ,$$

thus enhancing the emission from the O $2p$ valence band.

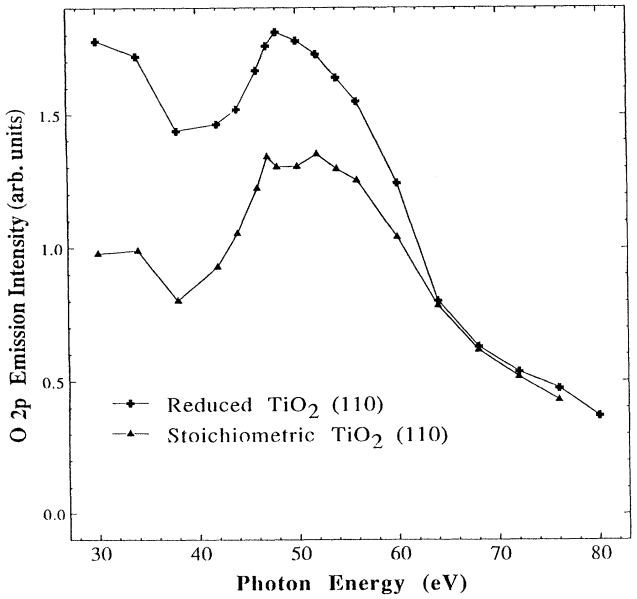

FIG. 3. Photon energy dependence of the total O $2p$ valence-band emission intensity from both stoichiometric and reduced TiO_2 (110) surfaces.

This mechanism was first proposed by Bertel, Stockbauer, and Madey,[3] which they refer to as "cross autoionization." Such an interatomic deexcitation process is expected to be dominant only when no intra-atomic decay channels are available, since intra-atomic transitions have far higher transition probabilities than do interatomic transitions.[14]

Figure 4 shows the bulk density of states of TiO_2 from a tight-binding calculation by Munnix and Schmeits;[15] similar results were obtained by Halley, Michalewicz, and Tit[16] using the Vos model and the equation-of-motion method. The total density of states as well as partial oxygen and titanium densities of states and orbital-resolved densities of states from both oxygen (O z,y,x orbitals) and titanium (e_g and t_{2g} bands) are shown. The nonnegligible contributions of the Ti $3d$ orbitals to the oxygen valence band lie mainly in the higher-binding-energy region, as seen from the Ti partial density of states in the valence-band region. This is consistent with the molecular-orbital model,[11] which predicts stronger interaction between the Ti $3d$ orbitals and the O $2p$ bonding orbitals lying in the higher-binding-energy region of the valence band. Therefore, the above model for resonant photoemission suggests that the higher-binding-energy region of the oxygen valence band, where the bonding orbitals have a larger admixture of Ti $3d$ character, should resonate more strongly than the nonbonding orbitals in the lower-binding-energy region of the valence band. [Although Ref. 15 is a bulk calculation, it has been shown by the same authors that the electronic structure of the TiO_2 (110) surface is essentially the same as that of the bulk,[15,17] and experimentally no surface states are

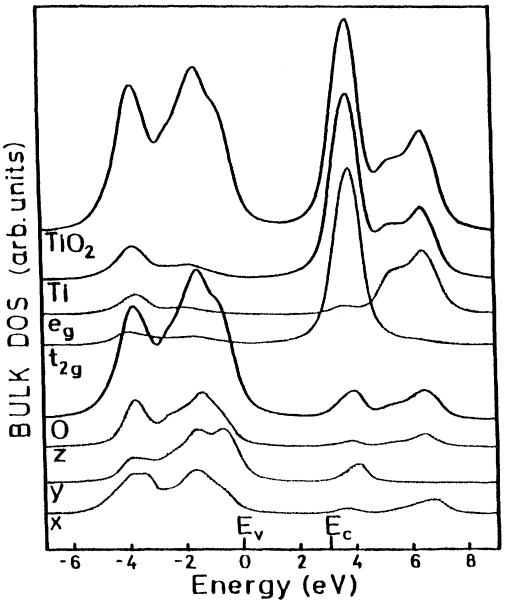

FIG. 4. Bulk density of states of TiO_2, together with partial oxygen and titanium densities of states. O partial DOS's are decomposed into O z,y,x orbital contributions, and Ti partial DOS's are decomposed into subbands of e_g ($3z^2-r^2, xy$) and t_{2g} (xz, yz, x^2-y^2) symmetry (Ref. 15).

detected in the bulk-band-gap region.[18] Therefore it is reasonable to compare our results with the bulk band calculations.]

In order to separate the contributions of the bonding and nonbonding orbitals to the valence-band resonant photoemission for comparison with theory, the spectra in the valence-band region were fitted with three Gaussians, which was the smallest number that gave a reasonable fit to all of the spectra. A nine-parameter nonlinear least-squares fitting program was used. Local chi squared minima were determined by using the inverse Hessian method.[19] Since there are many local minima in such a procedure, the solution is not unique. However, in order to get results that could be meaningfully compared among the different spectra, a common set of peak positions and peak widths for all the spectra should be used. Although it was impossible to get exactly the same peak positions and widths for all of the spectra due to the nature of the iterations, after numerous attempts the deviation was within 0.18 eV in peak positions, and within 0.13 eV in peak widths. A typical fit is shown in Fig. 5. Since the fitting procedure simply reproduces the experimental data and is not based upon theoretical considerations, none of the peaks from curve fitting will correspond to pure bonding or nonbonding orbitals. However, the highest-binding-energy peak should represent emission *predominantly* from the *bonding* orbitals, while the lowest-binding-energy peak corresponds to emission *predominantly* from the *nonbonding* orbitals; for convenience we shall refer to these as "bonding" and "nonbonding" orbital emission. The central peak consists of a combination of the two and will not be considered further here.

Figure 6(a) shows the photon energy dependence of the integrated intensity of the bonding and nonbonding peaks for a stoichiometric TiO_2 (110) surface (plotted on the same absolute scale). Measurements were made on several different TiO_2 (110) surfaces and, although the detailed dependence of the integrated intensity on photon energy varied somewhat from sample to sample, the energy locations and the general trends in amplitudes were the same. The differences between the resonant behavior of the bonding and nonbonding peaks can be seen more clearly in Fig. 6(b), where the same resonance profiles have been scaled so that their amplitudes coincide at photon energies of 64–68 eV. The O $2p$ bonding orbital emission intensity is seen to rise sharply at the onset of the Ti $3p \rightarrow 3d$ resonance, reach a maximum at approximately 47 eV photon energy, and fall off for photon energies above 47 eV. The cross-autoionization mechanism arising from cation-ligand mixing can account for the bonding orbital resonant behavior, since the Ti $3d$–O $2p$ hybridization is theoretically predicted to involve primarily those bonding orbitals, as discussed above. This is supported by the fact that the resonance profiles for the O $2p$ bonding orbitals in both stoichiometric and reduced TiO_2 are similar to that for the defect-induced Ti $3d$ states in reduced TiO_2, as shown in Fig. 7. All of the resonance profiles rise relatively sharply to a maximum at 47–48 eV and then fall off more gradually for higher photon energies.

Interestingly, emission from the O $2p$ nonbonding orbitals, which are predicted to hybridize only weakly with Ti $3d$ orbitals,[15,16] resonates as well, although not as strongly as that from the bonding orbitals [Fig. 6(b)]. In contrast to the bonding orbitals, the resonance profile for

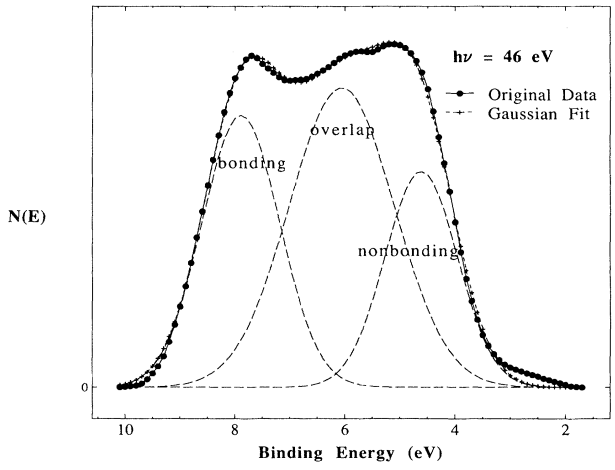

FIG. 5. Gaussian fit of the O $2p$ valence-band photoemission spectrum from stoichiometric TiO_2 (110) taken at 46 eV photon energy. See text for details.

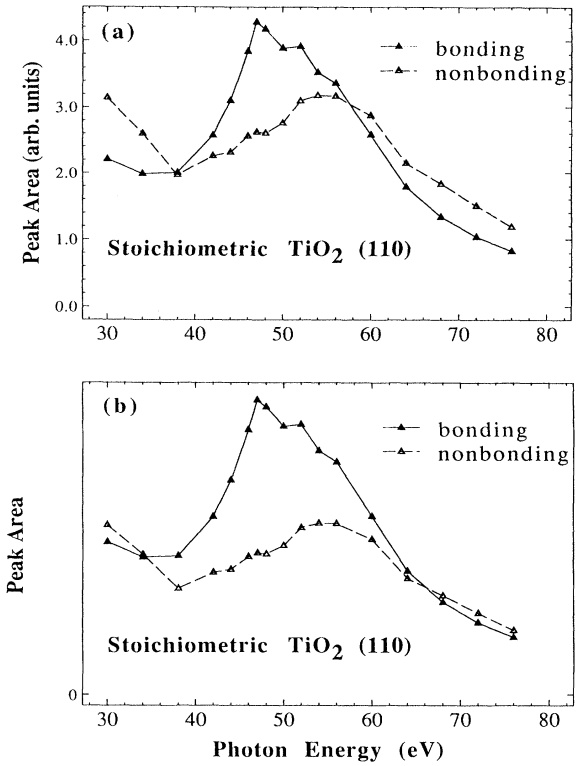

FIG. 6. Photon energy dependence of the O $2p$ bonding and nonbonding orbital emission intensity from stoichiometric TiO_2 (110): (a) original data, and (b) normalized at 64–68 eV.

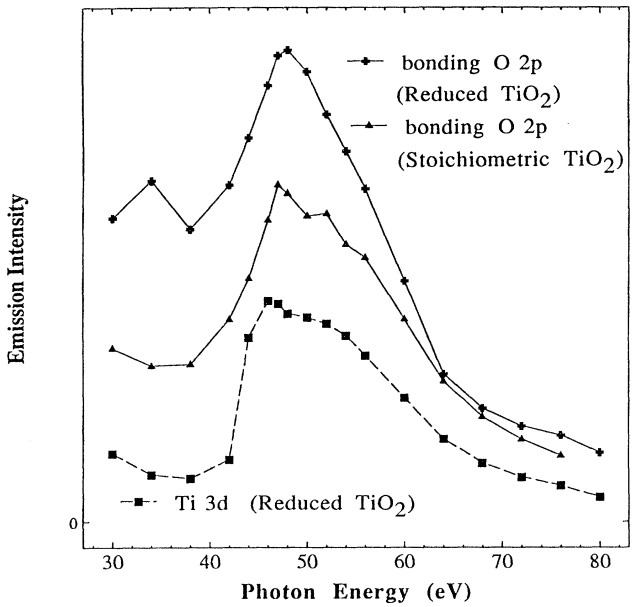

FIG. 7. Photon energy dependence of the O $2p$ bonding orbital emission intensity from both stoichiometric and reduced TiO_2 (110) and the Ti $3d$ emission intensity from reduced TiO_2 (110).

the nonbonding O $2p$ orbitals consists of a more gradual rise at the onset of the Ti $3p \rightarrow 3d$ resonance, a shoulder at about 47 eV photon energy, and a continuing rise until 54–56 eV photon energy. Thus the nonbonding O $2p$ orbital resonant behavior probably does not result primarily from Ti $3d$–O $2p$ mixing, as is the case for the bonding orbital resonance (although there should still be a small contribution from Ti $3d$–O $2p$ mixing). Since no optical transitions exist for oxygen ions in this photon energy range, the O $2p$ nonbonding orbital resonance must still arise from covalent mixing with Ti states; the shape of the resonance profile indicates that those states lie 7–9 eV above the Ti $3d$ band.

The energy spacing between the Ti $3d$ and Ti $4s$ orbitals in TiO_2 is around 8 eV, as determined from uv reflectivity,[20] x-ray absorption spectroscopy (XAS),[11,21–24] and electron-energy-loss spectroscopy (EELS) data,[10,23] and the hybridization between Ti $4sp$ and O $2p$ is reported by de Groot *et al.*[24] to be important in transition-metal oxides. (The Ti $4p$ states should not play any role in the resonant processes discussed here since the $3p \rightarrow 4p$ transition is dipole forbidden.) According to the molecular-orbital picture of an octahedrally coordinated cation in bulk TiO_2,[11] the nonbonding valence-band orbitals have no admixture of Ti $4s$ character, since the only O $2p$ orbital bonding to Ti $4s$ is $2a_{1g}$, which lies in the highest-binding-energy region of the valence band. However, additional O $2p$–Ti $4s$ coupling would be expected to arise from the reduced symmetry at the surface. There are two different Ti sites on the rutile (110) surface; one is surrounded by five oxygen atoms and the other by six oxygen atoms. The local point-group symmetries around both Ti sites are lowered from D_{2h} in the bulk to C_{2v} on the surface. The reduced symmetry causes the t_{2u} nonbonding oxygen orbital to split into a_1, a_2, and b_2 orbitals for the sixfold-coordinated surface Ti sites; hence this nonbonding orbital should mix with Ti $4s$ orbitals at the surface, which have a_1 symmetry. (The reduced symmetry at the surface does not lead to any major change in the hybridization between the Ti $3d$ and O $2p$ bonding orbitals.) Therefore, we propose the following mechanism to account for the nonbonding orbital resonance. When the photon energy is greater than the Ti $3p \rightarrow 4s$ optical transition energy, some Ti $3p$ electrons are excited into the initially empty $4sp$ band:

$$\text{Ti } 3p^6 3d^0 4s^0 + h\nu \rightarrow \text{Ti } [3p^5 3d^0 4s^1]^* \ .$$

The only nonradiative decay channel for this $[3p^5 3d^0 4s^1]^*$ excited state is to transfer energy to the oxygen valence-band electrons through Ti $4s$–O $2p$ hybridization:

$$\text{Ti } [3p^5 3d^0 4s^1]^* + \text{O } 2p^6 \rightarrow \text{Ti } 3p^6 3d^0 4s^0 + \text{O } 2p^5 + e^- \ .$$

This additional channel interferes with the direct photoemission process:

$$\text{O } 2p^6 + h\nu \rightarrow \text{O } 2p^5 + e^- \ ,$$

leading to an enhanced emission from the O $2p$ orbitals that have mixed Ti $4s$ character. Similar processes involving Mo $4p \rightarrow 5sp$ transitions have been suggested in a recent resonant photoemission study of MoS_2 at the Mo $4p \rightarrow 4d$ absorption edge.[25] [It should be noted, however, that the final state in photoemission consists of an $(n-1)$-electron system, compared to n electrons in the ground state; this would also modify the cation-ligand hybridization. Therefore, a proper description of photoemission must include both the n-electron initial and $(n-1)$-electron final states.[26] Unfortunately such an excited-state calculation for photoemission from TiO_2 has not been published.]

Since the Ti $4s$ orbitals hybridize with the bonding O $2p$ orbitals as well, there should also be a similar, probably larger contribution of the Ti $3p \rightarrow 4s$ resonance to the bonding orbital emission. We propose that this is one of the main reasons that the resonant profiles extend to such high photon energies.

B. Resonant photoemission in reduced TiO_2

When the TiO_2 (110) surface is reduced by ion bombardment, the $3d$ orbitals of Ti ions adjacent to the O vacancies become partially populated, giving rise to a Ti $3d$ emission band in UPS spectra.[8,9] The photon energy dependence of the total O $2p$ valence-band emission (area above an integrated background) and the Ti $3d$ emission (area above a linear background) for a slightly reduced surface are shown in Figs. 3 and 7, respectively. The Ti $3d$ resonance profile has the characteristic Fano line shape;[27] it is very similar to those reported for Ti metal,[3] Ti_2O_3,[4] and $SrTiO_{3-x}$.[5] This indicates a strongly localized excited state. (Because the screening of the cation electron orbitals in the ground state is reduced in going from a metal to its oxides, the energy of the initial state in

$3p \rightarrow 3d$ photoabsorption is changed. In order for these Ti $3d$ resonance profiles to peak at the same photon energy for Ti and for its oxides, the energy of the excited state must change by the same amount; i.e., chemical shifts must be the same for both ground and excited states, which is only possible if the excited state is highly localized.[3,4] Similar, but weaker, resonant behavior is observed for the oxygen valence-band emission. Comparing the two profiles in Fig. 3 shows that the total O $2p$ valence-band emission intensity resonates more strongly for stoichiometric TiO_2.

The individual contributions to the O $2p$ emission from the bonding and nonbonding components of the Gaussian fits at different photon energies are plotted for reduced TiO_2 (110) in Fig. 8(a). In Fig. 8(b) the same resonance profiles have been normalized at photon energies of 64–68 eV [compare with Fig. 6(b)]. As in the case of stoichiometric TiO_2 (110), the O $2p$ bonding orbital emission intensity increases rapidly at the onset of the $3p \rightarrow 3d$ resonance, maximizing at around 47–48 eV photon energy, while the nonbonding orbital emission intensity does not begin to rise until about 47–48 eV photon energy, reaching a maximum at approximately 52–56 eV photon energy. The origin of both the bonding and nonbonding orbital resonant behavior for reduced TiO_2 is the same as that proposed for stoichiometric TiO_2 above, although the absence of a shoulder near 47–48 eV in the nonbonding orbital resonance profile suggests less hybridization of the Ti $3d$ orbitals with the nonbonding O $2p$ orbitals for reduced TiO_2.

Besides the defect-induced Ti $3d$ states just below E_F, Ar-ion bombardment of TiO_2 (110) leads to a reduction in the emission intensity from the O $2p$ nonbonding orbitals, while that from the bonding orbitals is increased, as shown in Fig. 9. [This is also seen in Fig. 8(a), although there the smaller relative amplitude of the nonbonding orbital emission for reduced TiO_2 results partially from a relatively narrower Gaussian peak used to fit the nonbonding region of the valence band.] This is consistent with previous results reported by Göpel *et al.*[28] (Note that the population of surface Ti $3d$ orbitals bends the band at the surface such that the O $2p$ valence band moves away from E_F by about 0.4 eV.) The reduction of emission from the nonbonding orbitals for reduced TiO_2 is consistent with a recent tight-binding extended Hückel calculation,[29] which predicts that, for an O-terminated TiO_2 (110) surface (see Fig. 3 in Ref. 9), removal of surface bridging oxygen ions decreases the emission from the lowest binding energy region of the valence band. This calculation also predicts that, due to a covalent interaction between the Ti atoms adjacent to oxygen vacancies, an occupied defect-induced band-gap state is formed at 0.7 eV below the bottom of the conduction band, as seen in Figs. 2 and 9. However, removal of surface bridging oxygen ions is not the only result of ion bombardment, since it produces a disordered surface that exhibits no LEED patterns. Munnix and Schmeits[30] have suggested subsurface oxygen vacancies to account for the defect-induced states lying in the bulk band gap; this idea has been supported by an angle-resolved x-ray photoemission spectroscopy (XPS) study,[31] but it is not consistent with recent ion scattering spectroscopy measurements on both stoichiometric and reduced TiO_2.[32]

The increase in emission from the bonding O $2p$ orbitals for the reduced surface suggests that there is more covalent mixing between the Ti and O ions for that surface

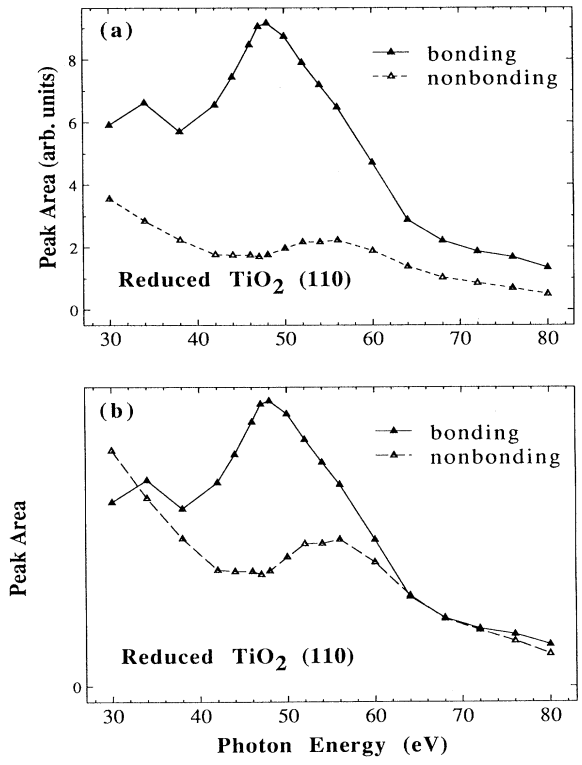

FIG. 8. Photon energy dependence of the O $2p$ bonding and nonbonding orbital emission intensity from reduced TiO_2 (110): (a) original data, and (b) normalized at 64–68 eV.

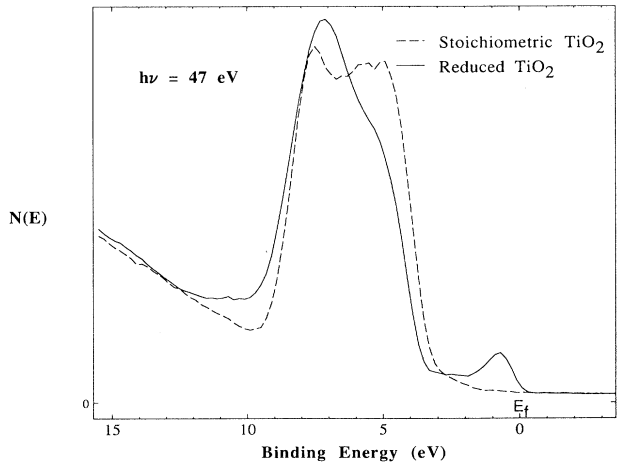

FIG. 9. UPS spectra from both stoichiometric and reduced TiO_2 (110) taken at 47 eV photon energy.

than for the stoichiometric one. This seems to contradict our experimental observation that the O $2p$ valence-band emission intensity resonates more for the stoichiometric TiO_2 (110) surface than for the reduced one, since more hybridization should lead to an increase in the amplitude of the O $2p$ resonance.[1] However, the resonant process discussed in Sec. III A above involves an *interatomic* deexcitation process, which should only make an appreciable contribution when no intra-atomic channels are available. Although partial population of the Ti $3d$ orbitals on the reduced surface may well increase the amount of O $2p$–Ti $3d$ hybridization, it also opens up the intra-atomic Auger decay channel for the $[3p^5 3d^{n+1}]^*$ intermediate state ($n \approx 1$ for Ti ions adjacent to O vacancies):

$$[3p^5 3d^2]^* \rightarrow 3p^6 3d^0 + e^- .$$

Since the cross section for this intra-atomic decay process is greater than that for the interatomic process[14] (which is the only nonradiative decay channel available for the stoichiometric surface), the latter process should become less probable for Ti ions adjacent to O-vacancy defect sites, resulting in a decrease in the resonant component of the O $2p$ emission.

Although one resonant photoemission study was reported for a thin TiO_2 surface layer on oxidized Ti, only bonding orbital resonant behavior was observed.[3] A possible explanation is that in that study the surface was not stoichiometric; some $3d$ emission existed in the spectra. As shown in Figs. 8(a) and 9, the major contribution to the oxygen valence-band photoemission in reduced TiO_2 is from the bonding orbitals; i.e., the emission intensity ratio of the bonding-to-nonbonding orbitals is very sensitive to Ti $3d$ population. Therefore, the amplitude of the resonance from nonbonding orbitals could be too small to be observed unless an effort was made to separate the bonding and nonbonding orbital contributions, as we have done here. Similar resonant enhancement from the lower-binding-energy part of the oxygen valence band was reported by Courths, Cord, and Saalfeld[5] in $SrTiO_3$ (001), although no energy shift in the peak position of the resonance profile was mentioned. An angle-resolved photoemission study was conducted to separate the bulk and surface contributions, from which they concluded that the resonant behavior of the lower-binding-energy region of the valence band resulted from enhanced surface covalency. The concept of enhanced surface covalency is similar to the increase in mixing between the lower-binding-energy region of the O $2p$ valence band and the Ti $4s$ states due to the reduced symmetry at the surface of TiO_2 (110) that was discussed above.

IV. SUMMARY

For both stoichiometric and reduced TiO_2 (110) surfaces, resonant photoemission from the O $2p$ valence band has been observed as the photon energy is swept through the cation $3p \rightarrow 3d$ optical-absorption edge at about 47 eV, indicating a strong cation-ligand hybridization. The emission intensity of the O $2p$ bonding orbitals exhibits a resonant profile similar to that of the Ti $3d$ orbitals on reduced surfaces; the origin of this resonance is ascribed to the covalent mixing between the Ti $3d$ band and O $2p$ bonding orbitals, which is consistent with the molecular-orbital model and the ground-state band calculations for bulk TiO_2. A weaker resonance for the nonbonding orbitals is observed for the first time to exhibit a maximum emission intensity at about 7 eV higher photon energy than the $3p \rightarrow 3d$ excitation threshold; the hybridization between the Ti $4s$ and O $2p$ nonbonding orbitals is proposed as the origin for this resonant behavior. The relative intensities of the O $2p$ bonding and nonbonding orbital emission are very sensitive to the Ti $3d$ population; partially populated Ti $3d$ states in reduced TiO_2 lead to more covalent mixing between the Ti $3d$ and O $2p$ orbitals. However, this enhanced covalency at surface defect sites is accompanied by a decreased amplitude of the oxygen valence-band resonance in reduced TiO_2; this occurs because the cross-autoionization process becomes less probable when intra-atomic decay channels become available.

ACKNOWLEDGMENTS

The authors would like to thank R. F. Garrett, G. P. Williams, and C. J. Hirschmugl of NSLS and K. E. Smith for their valuable help, K. M. Rabe for useful discussions, and J. S. Ledford for lending us his computer. This work was partially supported by the Department of Energy, Office of Basic Energy Sciences Grant No. DE-FG02-87ER13773, and by the National Science Foundation, Solid State Chemistry Grant No. DMR-87-11423. Research was carried out at the National Synchrotron Light Source, which is supported by the Department of Energy, Division of Materials Sciences and Division of Chemical Sciences Grant No. DE-AC02-76CH00016.

[1] L. C. Davis, J. Appl. Phys. **59**, R25 (1986), and references therein.

[2] A. Fujimori and F. Minami, Phys. Rev. B **30**, 957 (1984); G. A. Sawatzky and J. W. Allen, Phys. Rev. Lett. **53**, 2339 (1984); A. Fujimori, M. Saeki, N. Kimizuka, M. Taniguchi, and S. Suga, Phys. Rev. B **34**, 7318 (1986); R. J. Lad and V. E. Henrich, *ibid.* **39**, 13478 (1989).

[3] E. Bertel, R. Stockbauer, and T. E. Madey, Phys. Rev. B **27**, 1939 (1983); Surf. Sci. **141**, 355 (1984).

[4] K. E. Smith and V. E. Henrich, Phys. Rev. B **38**, 9571 (1988).

[5] R. Courths, B. Cord, and H. Saalfeld, Solid State Commun. **70**, 1047 (1989).

[6] N. B. Brooks, D. S.-L. Law, T. S. Padmore, D. R. Warburton, and G. Thornton, Solid State Commun. **57**, 473 (1986).

[7] S. Shin, S. Suga, M. Taniguchi, M. Fujisawa, H. Kanzaki, A. Fujimori, H. Daimon, Y. Ueda, K. Kosuge, and S. Kachi, Phys. Rev. B **41**, 4993 (1990).

[8] V. E. Henrich, G. Dresselhaus, and H. J. Zeiger, Phys. Rev. Lett. **36**, 1335 (1976).

[9] V. E. Henrich, Rep. Prog. Phys. **48**, 1481 (1985).

[10] L. A. Grunes, R. D. Leapman, C. N. Wilker, R. Hoffmann, and A. B. Kunz, Phys. Rev. B **25**, 7157 (1982).

[11]K. Tsutsumi, O. Aita, and K. Ichikawa, Phys. Rev. B **15**, 4638 (1977).
[12]J. A. Tossell, D. J. Vaughan, and K. H. Johnson, Am. Mineral. **59**, 319 (1974).
[13]B. Sonntag, R. Haensel, and C. Kunz, Solid State Commun. **7**, 597 (1969).
[14]J. A. D. Matthew and Y. Komninos, Surf. Sci. **53**, 716 (1975); C. N. R. Rao and D. D. Sarma, Phys. Rev. B **25**, 2927 (1982); S. Nishigaki, Surf. Sci. **125**, 762 (1983).
[15]S. Munnix and M. Schmeits, Phys. Rev. B **30**, 2202 (1984).
[16]J. W. Halley, M. T. Michalewicz, and N. Tit, Phys. Rev. B **41**, 10 165 (1990).
[17]S. Munnix and M. Schmeits, Phys. Rev. B **28**, 7342 (1983).
[18]V. E. Henrich and R. L. Kurtz, Phys. Rev. B **23**, 6280 (1981).
[19]See, for example, W. H. Press, B. P. Flannery, S. A. Teukolsky, and W. T. Vetterling, *Numerical Recipes* (Cambridge University Press, Cambridge, 1986), p. 521.
[20]M. Cardona and G. Harbeke, Phys. Rev. **137**, A1467 (1965).
[21]D. W. Fischer, Phys. Rev. B **5**, 4219 (1972).
[22]L. A. Grunes, Phys. Rev. B **27**, 2111 (1983).
[23]R. Brydson, H. Sauer, W. Engel, J. M. Thomas, E. Zeitler, N. Kosugi, and H. Kuroda, J. Phys. Condens. Matter. **1**, 797 (1989).
[24]F. M. F. de Groot, M. Grioni, J. C. Fuggle, J. Ghijsen, G. A. Sawatzky, and H. Petersen, Phys. Rev. B **40**, 5715 (1989).
[25]J. R. Lince, S. V. Didziulis, and J. A. Yarmoff, Phys. Rev. B **43**, 4641 (1991).
[26]G. A. Sawatzky, in *Core-Level Spectroscopy in Condensed Systems,* edited by J. Kanamori and A. Kotani (Springer-Verlag, Berlin, 1988), p. 99.
[27]U. Fano, Phys. Rev. **124**, 1866 (1961).
[28]W. Göpel, J. A. Anderson, D. Frankel, M. Jaehnig, K. Phillips, J. A. Schäfer, and G. Rocker, Surf. Sci. **139**, 333 (1984).
[29]C.-R. Wang and Y.-S. Xu, Surf. Sci. **219**, L537 (1989).
[30]S. Munnix and M. Schmeits, Phys. Rev. B **31**, 3369 (1985).
[31]U. Bardi, K. Tamura, M. Owari, and Y. Nihei, Appl. Surf. Sci. **32**, 352 (1988).
[32]T. E. Madey (private communication).